

1 **Title:** The evolution of the equatorial Pacific zonal SST gradient during the twentieth century

2

3 **Authors:**

4 Kristopher B. Karnauskas

5 Richard Seager

6 Alexey Kaplan

7 Yochanan Kushnir

8 Mark A. Cane

9

10 Lamont-Doherty Earth Observatory, Columbia University, Palisades, New York

11

12 2008.2.22 Manuscript submitted to the *Journal of Climate*

13

14 **Corresponding author's address:**

15 Dr. Kristopher B. Karnauskas

16 Lamont-Doherty Earth Observatory

17 Columbia University

18 301F Oceanography Bldg.

19 P.O. Box 1000 / 61 Route 9W

20 Palisades, NY 10964

21 (845) 365-8795

22 krisk@ldeo.columbia.edu

23 **Abstract:**

24 Two popular reconstructions of observed sea surface temperature, HadISST1 and NOAA  
25 ERSST (recently released version 3), are analyzed to clarify the evolution of the equatorial  
26 Pacific zonal SST gradient over the period 1880-2005. A brief survey of recently published  
27 analyses illustrates the widespread disagreement over the observed change in the SST gradient,  
28 which has implications for its projected response to global warming. Differences exist between  
29 the two reconstructions, but our straightforward analyses show that the observations allow us to  
30 be confident of three things: (1) the western equatorial Pacific has been warming, (2) the eastern  
31 equatorial Pacific has not been warming as much as the west, and (3) the equatorial Pacific zonal  
32 SST gradient has not been weakening. Rather, the observations suggest that the mean SST in the  
33 eastern equatorial Pacific has remained quite steady. Remaining uncertainties, however, prohibit  
34 making a stronger statement such as that the SST gradient has been strengthening.

35 The observational results are compared with and discussed in the context of IPCC AR4  
36 model simulations of the twentieth century climate and beyond. Five of the six models analyzed  
37 indicate a strengthening of the zonal SST gradient over the 20<sup>th</sup> century, while the GFDL CM2.1  
38 exhibits a substantial weakening of the zonal SST gradient caused by a large warming in the east.  
39 Beyond the 20<sup>th</sup> century, there is no convergence of results among the six models regarding the  
40 response of the zonal SST gradient to a continued increase of atmospheric CO<sub>2</sub> concentration.

## 41 **1. Introduction**

42           The basic pattern of sea surface temperature (SST) in the equatorial Pacific Ocean is  
43 characterized by a vast warm pool in the west, and a relatively narrow band of cold surface water  
44 extending westward from the coast of South America. The result is a rather linear zonal SST  
45 gradient of roughly  $-0.04^{\circ}\text{C}$  per degree longitude (Figure 1). Variations in this pattern, which  
46 occur strongly on interannual and decadal timescales, cause measurable climate variations  
47 around the world transmitted through the large-scale atmospheric circulation. During the  
48 twentieth century, the Earth was subject to unprecedented radiative forcing driven by rising  
49 anthropogenic carbon dioxide emissions. If rising greenhouse gases cause a change in the  
50 equatorial Pacific zonal SST gradient, it will impact the pattern of associated global climate  
51 change. A change of just a fraction of the zonal SST gradient is important because the Dust  
52 Bowl in the 1930s and other major droughts were caused by persistent changes in the SST  
53 gradient by such amounts (Schubert et al. 2004a, b; Seager et al. 2005, Herweijer et al. 2006).  
54 Therefore, it is worth examining equatorial Pacific climate change over the past century,  
55 particularly its response to radiative forcing and how well the response is represented in models  
56 used for future climate change projection.

57           Unlike models, nature has only one realization, and there are three possibilities as to what  
58 that realization has been. Either (1) the SST gradient has been strengthening, (2) trends in SST  
59 have been zonally uniform and thus the SST gradient has not been changing, or (3) the SST  
60 gradient has been weakening. What prevents universal agreement upon nature's single  
61 realization is the fact that observations of nature are imperfect. Several attempts have been made  
62 at characterizing twentieth century changes in the equatorial Pacific zonal SST gradient using  
63 observations. Using the Kaplan et al. (1998) SST data set, which is based on monthly anomalies

64 from the United Kingdom Meteorological Office historical SST data set MOHSST5 (Parker et al.  
65 1994), Cane et al (1997) and Cane (2005) showed that the linear trend in the east-central  
66 equatorial Pacific SSTs from 1900-1991 is negative (cooling), while in the western equatorial  
67 Pacific the trend is positive (warming), and thus the zonal SST gradient is strengthening. The  
68 analysis of Latif et al. (1997) of the GISST data set (Rayner et al. 1996), based on a newer  
69 version of the data set of historical SST observations MOHSST6, indicated that the linear trend  
70 in SST between 1949-1991 is highly uniform within 10° latitude of the equator, with the  
71 exception of a localized relative minimum warming (but not cooling) at 140°W. The results of  
72 Latif et al. (1997) therefore suggest no change in the zonal SST gradient. More recently, Liu et  
73 al. (2005) analyzed the HadISST1 data set (Rayner et al. 2003) and showed greater warming in  
74 the eastern equatorial Pacific than in the west over 1940-2000, and claimed that similar results  
75 could be obtained with other data sets, including the Kaplan et al. (1998) data set. Liu et al.  
76 (2005) therefore suggests a weakening of the zonal SST gradient.

77 Finally, Vecchi and Soden (2007) compared maps of the linear trends from the  
78 HadISST1, Kaplan et al. (1998), and NOAA Improved Extended Reconstruction of SST version  
79 2 (NOAA ERSST v.2; Smith and Reynolds 2004) data sets over 1880-2005. HadISST1 and  
80 Kaplan et al. (1998) indicated weak cooling (approx. -0.25°C per 125 years) in the eastern and  
81 central equatorial Pacific, and warming (approx. 0.5°C per 125 years) in the western equatorial  
82 Pacific. In contrast, NOAA ERSST v.2 indicated strong warming in the eastern and central  
83 equatorial Pacific (up to 1°C per 125 years), and much weaker warming (~0.25°C per 125 years)  
84 in the western equatorial Pacific. Therefore, based on the spatial maps of linear trends in Vecchi  
85 and Soden (2007), the HadISST1 and Kaplan et al. (1998) reconstructions would seem to be

86 consistent with a strengthening of the zonal SST gradient, while the NOAA ERSST v.2  
87 reconstruction suggests a weakening of the zonal SST gradient.

88         Despite the perceived importance of the distinction, there remains considerable  
89 disagreement on the response of the equatorial Pacific zonal SST gradient over the twentieth  
90 century to global warming. Mechanistic theories have been constructed to explain or justify both  
91 a strengthening SST gradient (e.g., Clement et al. 1996) and a weakening SST gradient (e.g.,  
92 Held and Soden 2006). Which of these mechanisms dominates the response is important to  
93 climate change because the former implies a delayed response on the timescale, potentially  
94 decadal or longer, over which the temperature of the water upwelled at the equator adjusts to the  
95 surface warming. Determining the nature of the response is difficult because of inconsistencies  
96 among aspects of the observational analyses of the twentieth century evolution of the mean state  
97 of the equatorial Pacific Ocean. To date, no attempt has been made to summarize what general  
98 conclusions of climatic importance can and cannot be safely extracted from the observations.  
99 Trends computed over different temporal periods can be difficult to interpret, and the use of  
100 spatial maps of linear trends can potentially mask some important aspects of the variability. The  
101 aim of this note is to provide a simple and uniform analysis of the twentieth century evolution of  
102 the equatorial Pacific zonal SST gradient using minimal temporal filtering, minimal dependency  
103 on such choices as spatial domains over which to average variables, and disclosure of the time  
104 evolution of the data behind such statistics as linear trends. Section 2 briefly describes the data  
105 sets and analysis methods used, and Section 3 is a presentation of the results, including  
106 comparisons with coupled models forced by observed and projected greenhouse gases. The  
107 paper concludes in Section 4 with a summary and discussion.

108

109 **2. Data and methodology**

110 *a. Data sets and models*

111 In this paper, we focus on tropical Pacific SSTs from the 1880s to the 2000s. For SSTs  
112 beginning in the late 1800s, we use two popular data sets: the U.K. Hadley Centre sea ice and  
113 temperature data set version 1 (HadISST1; Rayner et al. 2003), and the recently released NOAA  
114 Improved Extended Reconstruction of SST version 3 (NOAA ERSST v.3; Smith et al. 2008).  
115 HadISST1 replaced GISST version 2.3b in 2002, and NOAA ERSST v.3 very recently replaced  
116 NOAA ERSST v.2 (Smith and Reynolds 2004). Of the handful of SST reconstructions presently  
117 used within the climate community, we have chosen the Hadley Centre and NOAA data sets  
118 because they differ significantly in their analysis methods and bias corrections to the  
119 observations, and because they have been shown to produce very different portrayals of the  
120 historical evolution of the equatorial Pacific zonal SST gradient (e.g., Vecchi and Soden 2007  
121 who used the now superseded NOAA ERSST v.2). However, no such analyses using the NOAA  
122 ERSST v.3 data set have been presented to date. For comparison with modern SST, we use the  
123 satellite and *in situ*-based NOAA Optimal Interpolation version 2 (NOAA OI v.2; Reynolds et al.  
124 2002). The NOAA OI v.2 is based on *in situ* (ship and buoy) and satellite derived SSTs, and is  
125 widely considered to be the best SST product covering the 1980s to the present.

126 In the following section, we also compare our observational results with outputs from a  
127 handful of coupled general circulation models (CGCMs) included in the Fourth Assessment  
128 Report of the Intergovernmental Panel on Climate Change (IPCC AR4). We analyze six  
129 CGCMs, which were chosen based on the criterion that the ocean components of the CGCMs  
130 should be of reasonably high spatial resolution ( $\sim 1^\circ$ ). These models are the NCAR CCSM3.0,  
131 NOAA GFDL CM2.0 and CM2.1, U.K. Met Office HadCM3 and HadGEM1, and the University

132 of Tokyo CCSR MIROC3.2h (Table 1). For comparison with the observational reconstructions,  
133 we analyze the first two available runs of the Climate of the 20<sup>th</sup> Century experiment (20C3M),  
134 which is an experiment initialized at a stable pre-industrial state, and forced by the historical  
135 record of greenhouse gases, aerosols, volcanoes, and solar forcing. The exception is that only  
136 one 20C3M run from the MIROC3.2h is available.

137 To illustrate what these six CGCMs project for the future, we also show their results from  
138 the A1B scenario of the IPCC Special Report on Emissions Scenarios (SRES-A1B). The SRES-  
139 A1B scenario is thought to be a ‘middle of the road’ scenario in terms of CO<sub>2</sub> emissions,  
140 corresponding to low population growth, very high GDP growth, very high energy use, low land-  
141 use changes, medium resource availability, and rapid introduction of new and efficient  
142 technologies. In the SRES-A1B experiments, the CGCMs were initialized with the end of the  
143 20C3M experiments and integrated through the twenty first century with atmospheric CO<sub>2</sub>  
144 concentration increasing approximately linearly to 720 ppm (roughly equivalent to a doubling of  
145 the CO<sub>2</sub> present in the year 2000). Beyond the year 2100, CO<sub>2</sub> was held fixed at 720 ppm. We  
146 analyze the single available SRES-A1B run from each model from January 2001 through  
147 December 2199, with the exception that outputs from the CCSM3.0 and MIROC3.2h are only  
148 available through the year 2099. All model outputs were obtained from the World Climate  
149 Research Program (WCRP) Climate Model Intercomparison Project 3 (CMIP3) Multi-Model  
150 database (<https://esg.llnl.gov:8843>).

151

### 152 *b. Analysis methods*

153 Our analysis methods are quite simple. We first aim to characterize changes in the  
154 climatically important features of the mean state of the equatorial Pacific Ocean. Figure 1 shows

155 the long-term mean SST field of the tropical Pacific Ocean, and two boxes over which spatial  
156 average SST indices are computed. The two boxes, which are both of equal size and centered on  
157 the equator, capture the bulk of the climatically important features at the extrema of the zonal  
158 SST gradient: the western Pacific warm pool and the eastern Pacific cold tongue. Beginning  
159 with the monthly mean data from the reconstructions and model outputs, decadal mean SST  
160 indices are generated for both regions. Here we analyze total SST values, thus avoiding potential  
161 problems associated with choosing a climatology for computing monthly anomalies.

162 In addition to defining the western and eastern SST indices, we quantify the zonal SST  
163 gradient. We employ a method that utilizes the data available at all longitudes of the equatorial  
164 Pacific Ocean, which yields a quantity more aptly defining a gradient, without the traditional  
165 dependency on the exact bounds of the boxes used in spatial averaging. Note that a gradient  
166 minimizes the effect of systematic data corrections that may affect a time series at a single  
167 location. The method of calculating the zonal SST gradient is illustrated graphically in Figure 1  
168 (right panel). An equatorial SST  $SST_{EQ}$  is computed at each longitude by averaging SST  
169 between  $2.5^{\circ}S$  and  $2.5^{\circ}N$ . Next, a line is fit to  $SST_{EQ}(x)$  between  $140^{\circ}E$  and  $80^{\circ}W$  using the  
170 least-squares method. The slope of that line defines the zonal gradient of equatorial SST across  
171 the Pacific Ocean.

172

### 173 **3. Results**

#### 174 *a. Observations*

175 Shown in Figure 2 are the time series of decadal mean SST in the western and eastern  
176 equatorial Pacific from HadISST1 and NOAA ERSST v.3. In the west (left column), the two  
177 reconstructions are in close agreement, including interdecadal variability (correlation 0.84). Also

178 shown as triangles on the time series in Figure 2 are index values computed from NOAA OI v.2  
179 (matching periods and domains). In the west, HadISST1 is reasonably close to NOAA OI v.2 in  
180 the 1990s and 2000s (within  $0.1^{\circ}\text{C}$ ), and NOAA ERSST v.3 is a near-perfect match to NOAA OI  
181 v.2. In both reconstructions, a positive trend is evident and significant at the 90% confidence  
182 level, which is not affected by omitting data prior to 1900. The magnitude and significance of  
183 trends are listed in Table 2. Based on the data, one can conclude that SST in the western  
184 equatorial Pacific has been significantly warming over the twentieth century, which does not  
185 contradict any previously published analysis of observations known to the authors.

186 In the eastern equatorial Pacific (Figure 2, right column), there is less agreement between  
187 the reconstructions (correlation 0.68). There is agreement, in terms of absolute SST, in the  
188 middle of the twentieth century (the 1940s through the 1970s), but before (after) that period  
189 NOAA ERSST v.3 is generally colder (warmer). Strongly manifest in both reconstructions is the  
190 so-called climate shift of 1976-1977 (e.g., Trenberth 1990) which, in addition to a warmer  
191 overall equatorial SST, included a transition into a multidecadal period of increased frequency of  
192 El Niño events. Despite the large signal of the climate shift ( $\sim 0.5^{\circ}\text{C}$  in the mean absolute SST),  
193 the HadISST1 reconstruction shows no significant trend over 1880-2005. However, because of  
194 the shift, computing linear trends over the latter half of the twentieth century (cf. Latif et al.  
195 1997, Liu et al. 2005), emphasizes the warming in the east. In contrast, the NOAA ERSST v.3  
196 reconstruction shows a significant warming trend in the east over the period 1880-2005 ( $0.03^{\circ}\text{C}$   
197 per decade), which is nevertheless smaller than the trend in the west ( $0.05^{\circ}\text{C}$  per decade).  
198 Further, while the NOAA ERSST v.3 reconstruction is in near-perfect agreement with NOAA OI  
199 v.2 during the 1990s and 2000s in the west, it exhibits a warm bias in the east ( $\sim 0.2^{\circ}\text{C}$ ). This  
200 warm bias has a substantial effect on a linear trend fitted to the time series. If we replace the

201 decadal mean SST computed from NOAA ERSST v.3 in the 1990s and 2000s with that  
202 computed from NOAA OI v.2 (i.e., the triangles), the trend reduces to 0.0203°C per decade,  
203 which is not significant at the 90% confidence level. This fact, coupled with the lack of a  
204 significant trend in HadISST1, merits the conclusion that there is no significant warming trend in  
205 the eastern equatorial Pacific Ocean over the twentieth century.

206         The zonal SST gradient as depicted by HadISST1 and NOAA ERSST v.3 is shown in  
207 Figure 3. Consistent with the previous discussion of trends in the western and eastern equatorial  
208 Pacific, HadISST1 indicates a strengthening of the SST gradient of approximately 0.0003 °C  
209 °lon<sup>-1</sup> per decade, significant at the 90% confidence level. Such a trend is equivalent to a  
210 strengthening by 7% of the twentieth century mean gradient per century. In NOAA ERSST v.3,  
211 there is also a strengthening trend (but not a significant one, using the same confidence level). In  
212 both reconstructions, the 2000s (defined in this analysis as the six year period from January 2000  
213 through December 2005) saw the strongest mean equatorial Pacific zonal SST gradient on  
214 record. The comparison given in Vecchi and Soden (2007) of trends in the HadISST1, Kaplan  
215 SST, and NOAA ERSST v.2 (Smith and Reynolds 2004) reconstructions showed disagreement  
216 over the evolution of the SST gradient between the Hadley and Kaplan data sets on the one hand  
217 and the NOAA dataset on the other hand. However, using the most recent version of the NOAA  
218 data set, ERSST v.3 (Smith et al. 2008), suggests much less disagreement among the SST  
219 reconstructions. We therefore find it is safe to conclude that the equatorial Pacific zonal SST  
220 gradient has not been weakening over the twentieth century.

221

222 *b. Coupled models*

223           Given that CGCMs are among our primary tools for predicting the future evolution of the  
224 state of the climate system, especially in response to increasing radiative forcing, it is worthwhile  
225 to apply the analyses described above to the output from CGCMs that have a reasonably high  
226 ocean resolution (Table 1). Each 20C3M run effectively represents one model realization of the  
227 response of the twentieth century climate system to the observed rise in greenhouse gases, plus  
228 other forcing and any natural variability the model is capable of generating. Shown in Figures 4  
229 and 5 are time series of decadal mean SST in the western (left column) and eastern (right  
230 column) equatorial Pacific from each of the six models. Although the y-axis limits in Figures 4  
231 and 5 differ, the total range of each y-axis is 1.5°C, facilitating visual comparison among the  
232 models and with the observational depiction (Figure 2). In the west, the models show warming  
233 trends ranging from 0.04°C per decade (HadCM3) to 0.14°C per decade (MIROC3.2h) (all  
234 trends are listed in Table 2). The trend in MIROC3.2h is considerably higher than the next  
235 largest trend (0.08°C per decade; CM2.1) and appears to be an outlier. In the east, the models  
236 show warming trends ranging from 0.02°C per decade (HadGEM1) to 0.09°C per decade  
237 (CM2.1, MIROC3.2h). The CM2.1 and MIROC3.2h have the strongest warming trends in the  
238 east; they are approximately 3 times the trend in NOAA ERSST v.3.

239           Shown in Figures 6 and 7 (left column) are the model trends in the zonal SST gradient  
240 from the 20C3M experiment, computed in the same manner as for observations. The CCSM3.0,  
241 CM2.0, HadCM3, and HadGEM1 all show remarkably similar results in terms of the SST  
242 gradient: a slight strengthening consistent with the observations. The MIROC3.2h shows a  
243 larger strengthening (-0.0006 °C °lon<sup>-1</sup> per decade)<sup>1</sup>. Only the CM2.1 shows a weakening, but at

---

<sup>1</sup> The 20C3M runs from the medium resolution version of the MIROC3.2 were also analyzed, and produce nearly identical results as the high resolution version with regard to the west, east, and SST gradient indices.

244 0.0002 °C °lon<sup>-1</sup> per decade it is not significant at the 90% confidence level. Based on Figure 4,  
245 it is clear that the weakening trend in the CM2.1 comes from the large warming trend in the east.

246 Beyond the 20<sup>th</sup> century, the simulated SST gradients under the SRES-A1B scenario  
247 show no consistency (Figures 6 and 7, right column). We begin with the five CGCMs that  
248 indicated a strengthening SST gradient over the 20<sup>th</sup> century. Beyond the 20<sup>th</sup> century, the  
249 CCSM3.0 shows a continued slow and steady strengthening, the CM2.0 a slow and steady  
250 weakening, the HadCM3 a large weakening, the HadGEM1 neither, and the MIROC3.2h a very  
251 strong weakening similar in magnitude to its twentieth century strengthening. The large  
252 interdecadal variability in the CM2.1 makes it difficult to decipher any trend, but its evolution  
253 could be described as a ‘jump’ in the early-middle 21<sup>st</sup> century to a state of persistently stronger  
254 SST gradient. CGCMs do not appear helpful for predicting what the “A1B” extension to Figure  
255 3 (the observations) will look like. Regardless of what the six models showed for the twentieth  
256 century, under the SRES-A1B scenario, three predict a weakening of the SST gradient and two  
257 predict a strengthening of the SST gradient while the remaining model shows no significant  
258 trend. One model, the MIROC3.2h, gives an opposite sign of significant trends in the equatorial  
259 Pacific zonal SST gradient for the twentieth and twenty first centuries.

260 Vecchi et al. (2006) used the CM2.1 to illustrate a model weakening of the atmospheric  
261 overturning circulation in the twentieth century. It is interesting to note that, of the six models  
262 analyzed in this study, the CM2.1 is the only model whose 20<sup>th</sup> century trend in the SST gradient  
263 (although not significant at the 90% confidence level) is consistent, in the sense of the Bjerknes  
264 (1966) theory, with a weakening of the Walker circulation. Vecchi and Soden (2007) showed  
265 that *all* IPCC AR4 models indicate a weakening of the atmospheric overturning circulation in the  
266 SRES-A1B scenario. Since not all models show a weakening of the SST gradient in the SRES-

267 A1B scenario, this indicates that the coupling between the SST gradient and the Walker  
268 circulation may be more complex than envisaged by Bjerknes (1966).

269 It is also necessary to point out that none of the six CGCMs accurately reproduce the  
270 twentieth century mean state of the equatorial Pacific Ocean, which could limit the usefulness of  
271 their projections of that state beyond the twentieth century. Figure 8 indicates the range of  
272  $SST_{EQ}(x)$  from observations and models. Each of the six models has a cold bias of at least  $1^{\circ}\text{C}$   
273 in the western and central equatorial Pacific, and a warm bias of at least  $1^{\circ}\text{C}$  east of the  
274 Galápagos Islands. HadGEM1 has a particularly strong cold bias: note the range change if that  
275 model is excluded from the sample (Figure 8). The shapes of the  $SST_{EQ}(x)$  curves in the western  
276 equatorial Pacific suggest that the models lack a well-defined western Pacific warm pool, which  
277 is centered in observations at  $\sim 155^{\circ}\text{W}$ . In the east, the problems appear to be caused primarily  
278 by a lack of the coastal upwelling along South America connecting with the equatorial upwelling  
279 west of the Galápagos Islands.

280

#### 281 **4. Summary and discussion**

282 In this note, we have presented a simple and uniform analysis of the twentieth century  
283 evolution of SSTs in the western and eastern equatorial Pacific Ocean and the zonal gradient  
284 thereof. Given existing data uncertainties, observations allow us to conclude three things:

- 285 1. The western equatorial Pacific has been warming.
- 286 2. The eastern equatorial Pacific has not been warming as much as the west.
- 287 3. The equatorial Pacific zonal SST gradient has not been weakening.

288 An identical analysis applied to the Kaplan et al. (1998) SST reconstruction, extended to  
289 the present using the NOAA OI v.2 data set (Kaplan et al. 2003), yielded similar results (not

290 shown) to those of HadISST1. The strengthening trend of the zonal SST gradient in that data set  
291 is 14.6% smaller than that in HadISST1, but is significant at the 90% confidence level.

292 One of the fundamental challenges motivated by the results of this study is to understand  
293 why the eastern equatorial Pacific has not been warming as much as the western Pacific and  
294 other basins such as the tropical Indian and Atlantic Oceans (e.g., Cane et al. 1997; Cane 2005).  
295 This understanding is required for an assessment of the realism of model simulations of past and  
296 future climate changes. The results of this study remain too uncertain to confirm the so-called  
297 ocean dynamical thermostat mechanism proposed by Clement et al. (1996) and augmented by  
298 Cane et al. (1997) and Seager and Murtugudde (1997) (see also Sun and Liu 1996). While it is  
299 true that the SST gradient has not weakened, the theory for why the zonal SST gradient at the  
300 equator and Walker circulation should intensify in response to positive radiative forcing does not  
301 account for the solid reasons, later developed, based on analysis of the atmospheric energy  
302 budget, for why the tropical circulation should slow (Betts 1998, Held and Soden 2006, and  
303 Vecchi and Soden 2007) and, hence, reduce the SST gradient.

304 A consistent analysis of six state-of-the-art coupled climate models, each included in the  
305 IPCC Fourth Assessment Report, suggests that several of the models are capable of producing a  
306 20<sup>th</sup> century greenhouse warming-driven trend in the equatorial Pacific zonal SST gradient that is  
307 consistent with observations, while the CM2.1 in particular overestimates the warming trend in  
308 the east and therefore produces a weakening of the SST gradient. It is interesting to note that  
309 such varied results can be obtained from models with similar ocean resolutions. Apparently  
310 other model characteristics are more important than the spatial resolution of the ocean. In  
311 response to a continued rise in atmospheric CO<sub>2</sub> (the SRES-A1B scenario), there is no  
312 convergence of results for the change of the SST gradient in the six models analyzed. It is also

313 not encouraging that all of the models fail to reproduce the observed twentieth century mean  
314 state of the equatorial Pacific Ocean.

315         Interestingly, the twentieth century evolution of the equatorial Pacific zonal SLP gradient  
316 using reconstructions from the same institutions as presented herein (HadSLP2 [Allan and Ansell  
317 2006] and NOAA ERSLP [Smith and Reynolds 2004]) yields results that apparently contradict  
318 the SST products of the same institutions. Based on Figure 3, and our understanding of the  
319 coupling of the tropical ocean and atmosphere on interannual timescales, one might expect  
320 HadSLP2 to indicate a strengthening of the SLP gradient, indicative of a strengthening Pacific  
321 Walker circulation. However, when the SLP gradient is computed in the same manner as we  
322 computed the SST gradient, HadSLP2 yields a significant weakening trend of the SLP gradient  
323 roughly by 10% of the twentieth century mean equatorial SLP gradient per century. The latter  
324 result is consistent with previous analyses of observed SLP (e.g., Vecchi et al. 2006) and SOI  
325 (Doherty and Hulme 2002). The inconsistency between trends in the SST and SLP gradients  
326 raises major concerns over whether our understanding of coupled interannual variability (i.e., the  
327 Bjerknes feedback) can effectively translate to longer timescales such as the tropical climate's  
328 response to global warming.

329         A complete understanding of the tropical Pacific atmosphere-ocean response to radiative  
330 forcing has not yet been achieved. While the ocean-centric theory developed by Clement and  
331 coworkers ignores the constraints imposed by atmospheric and planetary energy balances, the  
332 atmosphere-centric theory developed by Vecchi, Soden and coworkers largely bypasses the  
333 possibility for changes in tropical ocean heat transport to modify the spatial pattern of SST  
334 response to forcing. A potentially fruitful way forward is to realize that the two theories need not  
335 be inconsistent with each other. There are two lines of argument for why global warming should

336 induce a weaker tropical circulation. The first follows from energy budget and moist  
337 thermodynamic constraints and notes that precipitation increases with temperature at a slower  
338 rate than does boundary layer atmospheric water vapor. Consequently the mass transport from  
339 the boundary layer into the free troposphere in regions of deep convection must decrease to  
340 enable both these constraints to be met. However, while this constraint implies a weakening  
341 tropical circulation, it applies to the circulation overall and need not imply a weaker Walker  
342 Circulation if the Hadley Cell is capable of accomplishing the balances on its own. The second  
343 line of argument notes that throughout the tropics away from regions of convection subsidence  
344 warming is balanced by radiative cooling. In a warmer atmosphere the static stability increases  
345 and, hence, the radiative cooling can be balanced by weaker subsidence, i.e., a weaker circulation  
346 (Betts 1998). However, the radiative cooling of the atmospheric column does increase in a  
347 warmer and moister atmosphere and will introduce a tendency to stronger subsidence that will  
348 offset the tendency to reduced subsidence imposed by increased static stability. More work  
349 remains to be done assessing how the tropical Pacific Ocean has responded to past radiative  
350 forcing, how well models represent this response, and how the Pacific Ocean will respond in the  
351 future. The range of oceanic, atmospheric and planetary energy balance constraints, which will  
352 determine the actual response, needs to be taken into account.

353 **Acknowledgements:**

354 The authors are grateful for the accessible archiving of climate model output by the WCRP  
355 CMIP3 Multi-Model database (<https://esg.llnl.gov:8843>), and acknowledge the NOAA climate  
356 data distribution web site (<http://www.cdc.noaa.gov/PublicData/>) and U.K. Met Office Hadley  
357 Center ‘HadObs’ web site (<http://hadobs.metoffice.com/>) for access to observational SST  
358 reconstructions. This work was supported by NSF grant ATM-04-17909 and NOAA grant  
359 NA030OAR4320179. LDEO contribution number XXXX.

360 **List of references:**

361 Allan, R. J. and Ansell, T. J., 2006: A new globally complete monthly historical mean sea level  
362 pressure data set (HadSLP2): 1850-2004, *J. Climate*, **19** 5816-5842.

363 Betts, A.K., 1998: Climate-convection feedbacks: Some further issues. *Climatic Change*, **39**, 35-  
364 38.

365 Bjerknes, J., 1966: The possible response of the atmospheric Hadley circulation to equatorial  
366 anomalies of ocean temperature. *Tellus*, **18**, 820-829.

367 Cane, M.A., A. C. Clement, A. Kaplan, Y. Kushnir, D. Pozdnyakov, R. Seager, S. E. Zebiak and  
368 R. Murtugudde. 1997: Twentieth-century sea surface temperature trends, *Science*, **275**, 957-960.

369 Cane, M.A., 2005: The evolution of El Niño, past and future, *Earth and Planetary Science*  
370 *Letters*, **230**, 227-240.

371 Collins, W.D., C.M. Bitz, M.L. Blackmon, G.B. Bonan, C.S. Bretherton, J.A. Carton, P. Chang,  
372 S.C. Doney, J.J. Hack, T.B. Henderson, J.T. Kiehl, W.G. Large, D.S. McKenna, B.D. Santer, and  
373 R.D. Smith, 2006: The Community Climate System Model Version 3 (CCSM3). *J. Climate*, **19**,  
374 2122–2143.

375 Clement A., R. Seager, M. A. Cane, and S. E. Zebiak, 1996: An ocean dynamical thermostat. *J.*  
376 *Climate*, **9**, 2190–2196.

377 Delworth, T.L., A.J. Broccoli, A. Rosati, R.J. Stouffer, V. Balaji, J.A. Beesley, W.F. Cooke,  
378 K.W. Dixon, J. Dunne, K.A. Dunne, J.W. Durachta, K.L. Findell, P. Ginoux, A. Gnanadesikan,

379 C.T. Gordon, S.M. Griffies, R. Gudgel, M.J. Harrison, I.M. Held, R.S. Hemler, L.W. Horowitz,  
380 S.A. Klein, T.R. Knutson, P.J. Kushner, A.R. Langenhorst, H.C. Lee, S.J. Lin, J. Lu, S.L.

381 Malyshev, P.C.D. Milly, V. Ramaswamy, J. Russell, M.D. Schwarzkopf, E. Shevliakova, J.J.

382 Sirutis, M.J. Spelman, W.F. Stern, M. Winton, A.T. Wittenberg, B. Wyman, F. Zeng, and R.

383 Zhang, 2006: GFDL's CM2 Global Coupled Climate Models. Part I: Formulation and Simulation  
384 Characteristics. *J. Climate*, **19**, 643–674.

385 Doherty, R.M., and M. Hulme, 2002: The relationship between the SOI and extended tropical  
386 precipitation in simulations of future climate change. *Geophys. Res. Lett.*, **29**(10), 113-114.

387 Gordon, C., C. Cooper, C. A. Senior, H. Banks, J. M. Gregory, T. C. Johns, J. F. B. Mitchell, and  
388 R. A. Wood, 2000: The simulation of SST, sea ice extents and ocean heat transport in a version  
389 of the Hadley Centre coupled model without flux adjustments. *Clim. Dyn.*, **16**, 147-168.

390 Held I. M., and B. J. Soden, 2006: Robust responses of the hydrological cycle to global warming.  
391 *J. Climate*, **19**, 5686–5699.

392 Herweijer, C., R. Seager, and E. R. Cook, 2006: North American droughts of the mid to late  
393 nineteenth century: a history, simulation and implication for Mediaeval drought. *Holocene*, **16**,  
394 159-171.

395 Hurrell, J.W., and K.E. Trenberth, 1999: Global Sea Surface Temperature Analyses: Multiple  
396 Problems and Their Implications for Climate Analysis, Modeling, and Reanalysis. *Bull. Amer.*  
397 *Meteor. Soc.*, **80**, 2661–2678.

398 Kaplan, A., M. Cane, Y. Kushnir, A. Clement, M. Blumenthal, and B. Rajagopalan, 1998:  
399 Analyses of global sea surface temperature 1856-1991, *J. Geophys. Res.*, **103**, 18,567-18,589.

400 Kaplan A., Y. Kushnir, M.A. Cane, 2000: Reduced space optimal interpolation of historical  
401 marine sea level pressure, *J. Climate*, **13**, 2987-3002.

402 Kaplan, A., M. A. Cane and Y. Kushnir, 2003: Reduced space approach to the optimal analysis  
403 interpolation of historical marine observations: Accomplishments, difficulties, and prospects,  
404 *Advances in the Applications of Marine Climatology: The Dynamic Part of the WMO Guide to*

405 the Applications of Marine Climatology, WMO/TD-1081. World Meteorological Organization,  
406 Geneva, Switzerland, pp. 199-216.

407 Latif, M., R. Kleeman, and C. Eckert, 1997: Greenhouse Warming, Decadal Variability, or El  
408 Niño? An Attempt to Understand the Anomalous 1990s. *J. Climate*, **10**, 2221–2239.

409 Liu, Z., S. Vavrus, F. He, N. Wen, and Y. Zhong, 2005: Rethinking Tropical Ocean Response to  
410 Global Warming: The Enhanced Equatorial Warming. *J. Climate*, **18**, 4684–4700.

411 Parker, D. E., P. D. Jones, C. K. Folland, and A. Bevan, 1994: Interdecadal changes of surface  
412 temperature since the late 19th century, *J. Geophys. Res.*, **99**, 14,377– 14,399.

413 Rayner, N. A., E. B. Horton, D. E. Parker, C. K. Folland, and R. B. Hackett, 1996: Version 2.2 of  
414 the Global Sea-Ice and Sea Surface Temperature data set, 1903–1994. CRTN 74, 21 pp. plus  
415 figures. [Available from Hadley Centre for Climate Prediction and Research, Meteorological  
416 Office, London Road, Bracknell, Berkshire, RG12 2SY, United Kingdom.]

417 Rayner N. A., D. E. Parker, E. B. Horton, C. K. Folland, L. V. Alexander, D. P. Rowell, E. C.  
418 Kent, and A. Kaplan, 2003: Global analyses of sea surface temperature, sea ice, and night marine  
419 air temperature since the late nineteenth century. *J. Geophys. Res.*, **108**, 4407,  
420 doi:10.1029/2002JD002670.

421 Reynolds, R.W., N.A. Rayner, T.M. Smith, D.C. Stokes, and W. Wang, 2002: An Improved In  
422 Situ and Satellite SST Analysis for Climate. *J. Climate*, **15**, 1609–1625.

423 Schubert, S. D., M. J. Suarez, P. J. Pegion, R. D. Koster, and J. T. Bacmeister, 2004a: Causes of  
424 long-term drought in the US Great Plains. *J. Climate*, **17**, 485-503.

425 Schubert, S.D., 2004b: On the cause of the 1930s Dust Bowl. *Science*, **303**, 1855-1859.

426 Seager, R., and R. Murtugudde, 1997: Ocean Dynamics, Thermocline Adjustment, and  
427 Regulation of Tropical SST. *J. Climate*, **10**, 521–534.

428 Seager, R., Y. Kushnir, C. Herweijer, N. Naik, and J. Velez, 2005: Modeling of tropical forcing  
429 of persistent droughts and pluvials over western North America: 1856-2000. *J. Climate*, **18**,  
430 4065-4088.

431 Smith T. M., and R. W. Reynolds, 2004: Improved extended reconstruction of SST (1854–1997).  
432 *J. Climate*, **17**, 2466–2477.

433 Smith, T.M., and R.W. Reynolds, 2004: Reconstruction of Monthly Mean Oceanic Sea Level  
434 Pressure Based on COADS and Station Data (1854-1997). *J. Oceanic Atmos. Tech.*, **21**, 1272-  
435 1282.

436 Smith, T.M., R.W. Reynolds, T.C. Peterson, and J. Lawrimore, 2008: Improvements to NOAA's  
437 Historical Merged Land-Ocean Surface Temperature Analysis (1880-2006). In press. *Journal of*  
438 *Climate*.

439 Sun, D.-Z. and Z. Liu, 1997: Dynamic ocean-atmosphere coupling: a thermostat for the tropics.  
440 *Science*, **272**, 1148-1150.

441 Vecchi, G. A., B. J. Soden, A. T. Wittenberg, I. M. Held, A. Leetmaa, and M. J. Harrison, 2006:  
442 Weakening of tropical Pacific atmospheric circulation due to anthropogenic forcing. *Nature*,  
443 **441**(7089), 73-76.

444 Vecchi, G.A., and B.J. Soden, 2007: Global Warming and the Weakening of the Tropical  
445 Circulation. *J. Climate*, **20**, 4316–4340.

446 Woodruff, S.D., R.J. Slutz, R.L. Jenne, and P.M. Steurer, 1987: A comprehensive ocean-  
447 atmosphere data set. *Bull. Amer. Meteor. Soc.*, **68**, 1239-1250.

448 **List of tables and figures:**

449 **Table 1.** List of coupled general circulation models (CGCMs) analyzed in the present study,  
450 including their zonal, meridional, and vertical ocean resolutions, and published reference.

451 **Table 2.** Linear trends of decadal mean: SST in the western and eastern equatorial Pacific ( $^{\circ}\text{C}$   
452 per decade), and the equatorial Pacific zonal SST gradient ( $^{\circ}\text{C } ^{\circ}\text{lon}^{-1}$  per decade) from  
453 observations, 20C3M experiments, and SRES-A1B experiments. Bold indicates statistical  
454 significance at the 90% confidence level, based on a two-tailed Student's t-test.

455 **Figure 1.** Left: observed twentieth century mean SST ( $^{\circ}\text{C}$ ) in the tropical Pacific Ocean from  
456 HadISST1. The shaded boxes denote areas over which SST indices are calculated and discussed  
457 in the main text (west:  $150^{\circ}\text{E}$ - $170^{\circ}\text{W}$ ,  $5^{\circ}\text{S}$ - $5^{\circ}\text{N}$ ; east:  $120^{\circ}\text{W}$ - $80^{\circ}\text{W}$ ,  $5^{\circ}\text{S}$ - $5^{\circ}\text{N}$ ). Right:  
458 corresponding equatorial SST ( $^{\circ}\text{C}$ ) as a function of longitude from HadISST1 and linear fit using  
459 the least-squares method.

460 **Figure 2.** Time series of observed decadal mean SST ( $^{\circ}\text{C}$ ) in the western (left column) and  
461 eastern (right column) equatorial Pacific Ocean from HadISST1 (top row) and NOAA ERSST  
462 v.3 (bottom row). Dashed lines represent linear trends, the magnitudes and significance of which  
463 are listed in Table 2. Triangles represent corresponding values from the NOAA OI v.2 data set.  
464 The decade marked 2000 includes January 2000 through December 2005.

465 **Figure 3.** Time series of observed decadal mean equatorial Pacific zonal SST gradient ( $^{\circ}\text{C } ^{\circ}\text{lon}^{-1}$   
466  $^{\circ}\text{lon}^{-1}$ ) from HadISST1 (left) and NOAA ERSST v.3 (right). Dashed lines represent linear trends, the  
467 magnitudes and significance of which are listed in Table 2. Triangles represent corresponding  
468 values from the NOAA OI v.2 data set. The decade marked 2000 includes January 2000 through  
469 December 2005.

470 **Figure 4.** Time series of simulated decadal mean SST ( $^{\circ}\text{C}$ ) in the western (left column) and  
471 eastern (right column) equatorial Pacific Ocean from the 20C3M experiment of the CCSM3.0  
472 (top row), CM2.0 (middle row), and CM2.1 (bottom row). Thin lines are individual realizations,  
473 and the heavy line is the mean. Dashed lines represent linear trends of the means.

474 **Figure 5.** As in Figure 4 but of the HadCM3 (top row), HadGEM1 (middle row), and  
475 MIROC3.2h (bottom row).

476 **Figure 6.** Time series of simulated decadal mean equatorial Pacific zonal SST gradient ( $^{\circ}\text{C }^{\circ}\text{lon}^{-1}$ )  
477  $^{\circ}\text{lon}^{-1}$ ) from the 20C3M (left column) and SRES-A1B (right column) experiments of the CCSM3.0  
478 (top row), CM2.0 (middle row), and CM2.1 (bottom row). Thin lines are individual realizations,  
479 and the heavy line is the mean. Dashed lines represent linear trends of the means.

480 **Figure 7.** As in Figure 6 but of the HadCM3 (top row), HadGEM1 (middle row), and  
481 MIROC3.2h (bottom row).

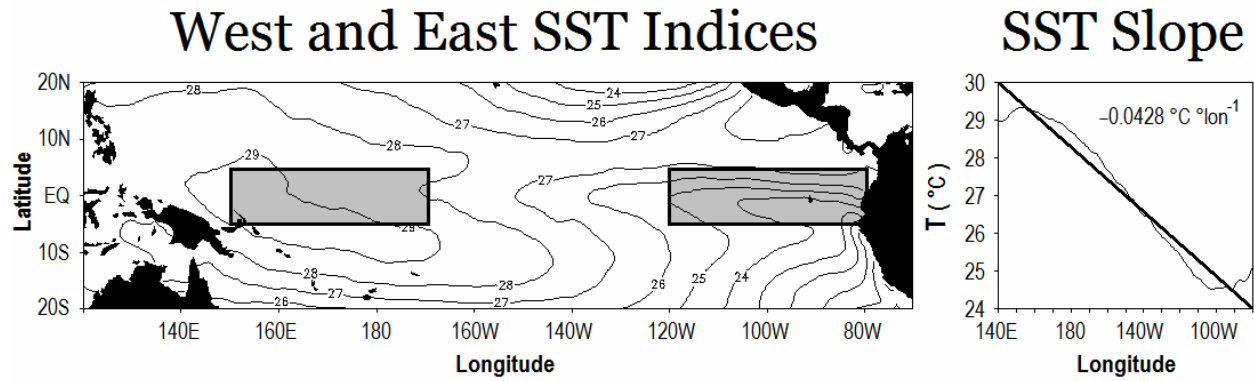
482 **Figure 8.** Range of observed (HadISST1 and NOAA ERSST v.3; black) and model simulated  
483 (gray) mean equatorial SST (averaged from  $2.5^{\circ}\text{S}$  to  $2.5^{\circ}\text{N}$ ;  $^{\circ}\text{C}$ ) as a function of longitude ( $^{\circ}\text{east}$ )  
484 over the twentieth century (January 1900 through December 1999). The light and dark grays  
485 together represent the range from all six CGCMs analyzed in the present study, and the light gray  
486 represents the range if HadGEM1 is excluded.

CGCM	Zonal	Meridional	Levels	Reference
NCAR CCSM3.0	1.1°	0.27-1°	40	Collins et al. 2006
NOAA GFDL CM2.0	1°	0.33-1°	50	Delworth et al. 2006
NOAA GFDL CM2.1	1°	0.33-1°	50	Delworth et al. 2006
UKMO HadCM3	1.25°	1.25°	20	Gordon et al. 2000
UKMO HadGEM1	1°	0.33-1°	40	Johns et al. 2006
CCSR MIROC3.2h	0.28°	0.19°	47	Hasumi and Emori 2004

488 **Table 1.** List of coupled general circulation models (CGCMs) analyzed in the  
489 present study, including their zonal, meridional, and vertical ocean resolutions,  
490 and published reference.

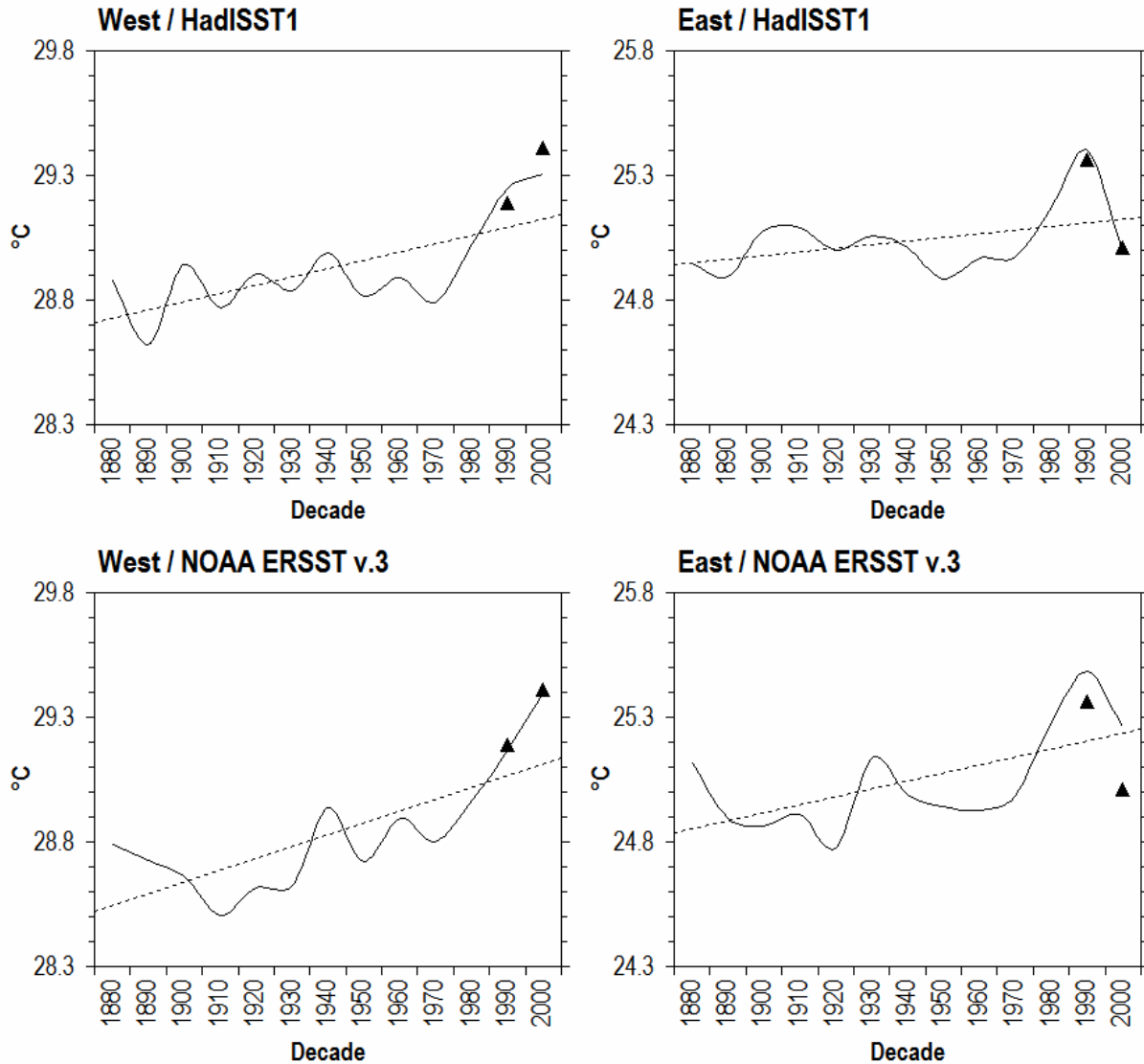
Reconstruction or CGCM	<i>1880s - 2000s or 20C3M</i>			<i>SRES-A1B</i>
	West	East	Gradient	Gradient
HadISST1	<b>0.03</b>	0.01	<b>-0.0003</b>	
ERSST v.3	<b>0.05</b>	<b>0.03</b>	-0.0001	
CCSM3.0	<b>0.05</b>	<b>0.05</b>	<b>-0.0001</b>	<b>-0.0001</b>
CM2.0	<b>0.06</b>	<b>0.06</b>	-0.0000	0.0001
CM2.1	<b>0.08</b>	<b>0.09</b>	0.0002	-0.0000
HadCM3	<b>0.04</b>	<b>0.03</b>	-0.0001	<b>0.0004</b>
HadGEM1	<b>0.05</b>	<b>0.02</b>	<b>-0.0003</b>	-0.0000
MIROC3.2h	<b>0.14</b>	<b>0.09</b>	<b>-0.0006</b>	<b>0.0007</b>

492 **Table 2.** Linear trends of decadal mean: SST in the western  
493 and eastern equatorial Pacific ( $^{\circ}\text{C}$  per decade), and the  
494 equatorial Pacific zonal SST gradient ( $^{\circ}\text{C } ^{\circ}\text{lon}^{-1}$  per decade)  
495 from observations, 20C3M experiments, and SRES-A1B  
496 experiments. Bold indicates statistical significance at the  
497 90% confidence level, based on a two-tailed Student's t-test.



498

499 **Figure 1.** Left: observed twentieth century mean SST (°C) in the tropical Pacific Ocean from  
 500 HadISST1. The shaded boxes denote areas over which SST indices are calculated and discussed  
 501 in the main text (west: 150°E-170°W, 5°S-5°N; east: 120°W-80°W, 5°S-5°N). Right:  
 502 corresponding equatorial SST (°C) as a function of longitude from HadISST1 and linear fit using  
 503 the least-squares method.



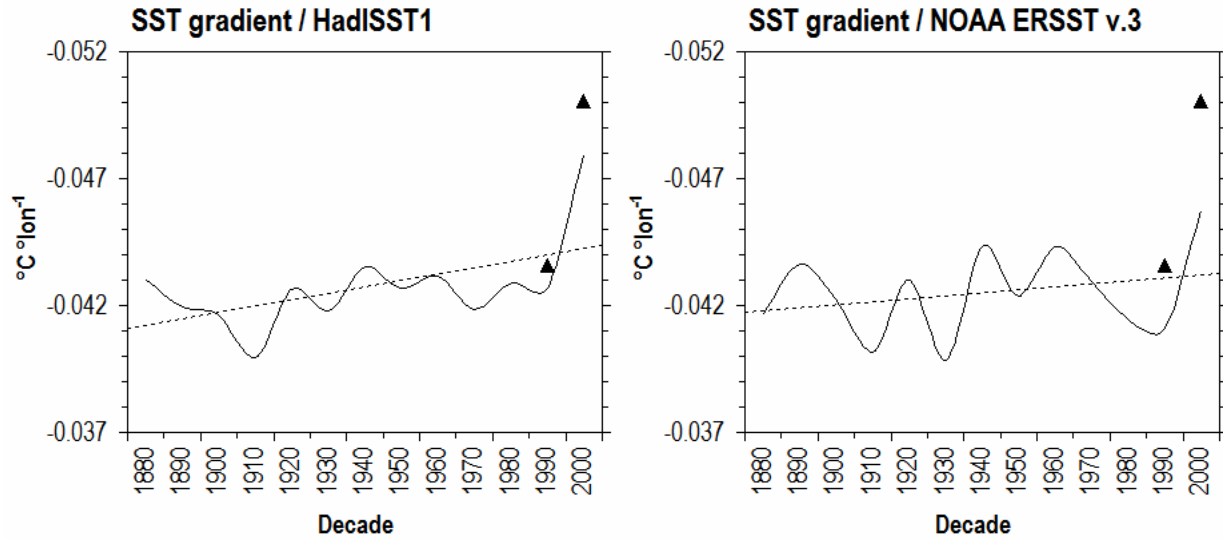
504

505 **Figure 2.** Time series of observed decadal mean SST (°C) in the western (left column) and  
 506 eastern (right column) equatorial Pacific Ocean from HadISST1 (top row) and NOAA ERSST

507 v.3 (bottom row). Dashed lines represent linear trends, the magnitudes and significance of which

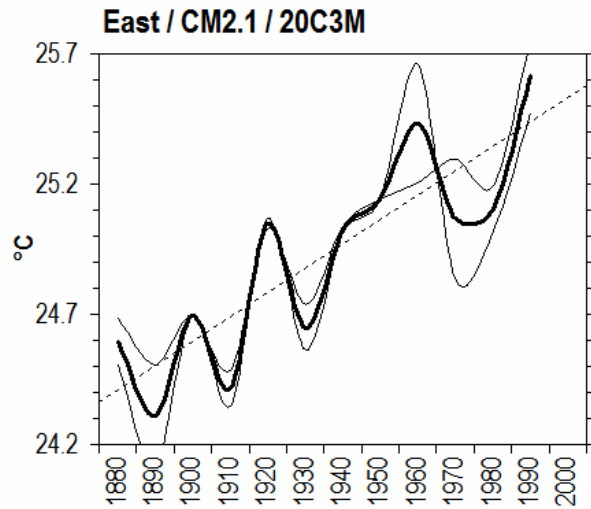
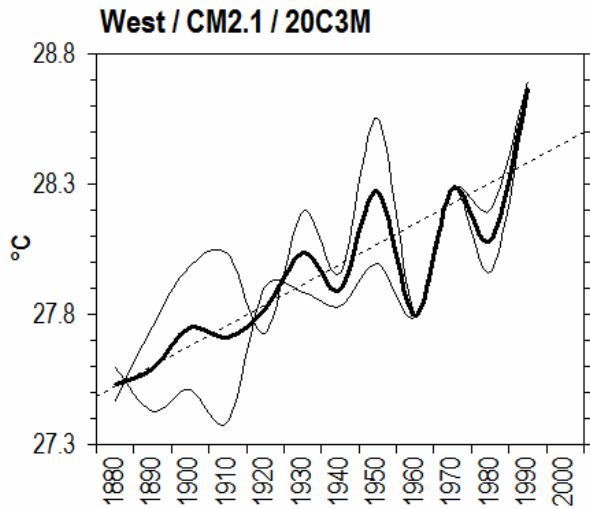
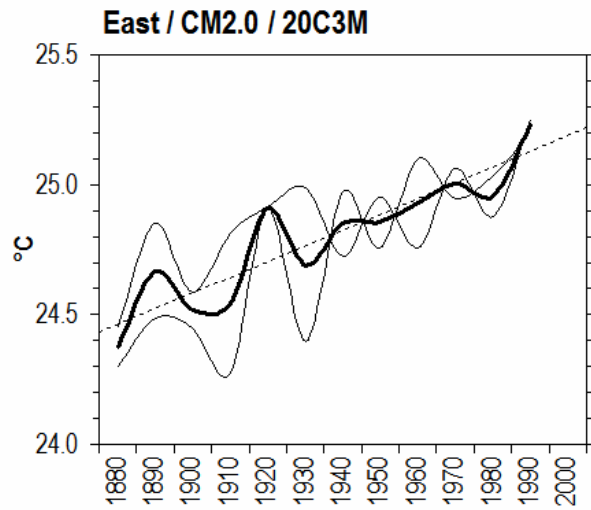
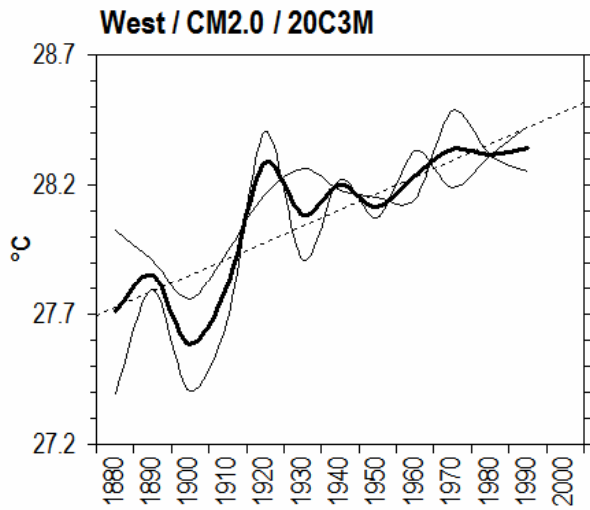
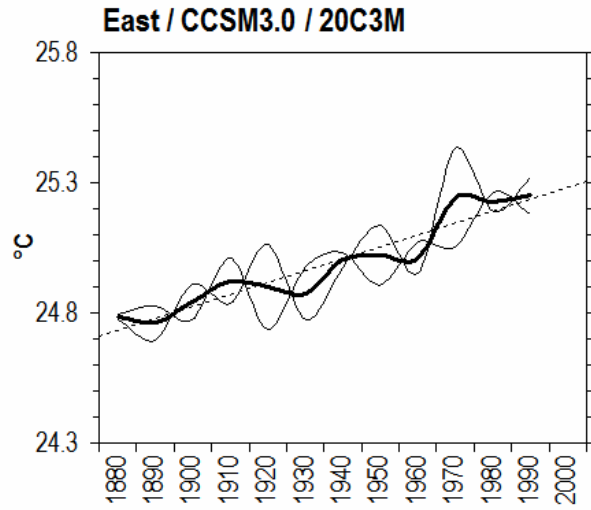
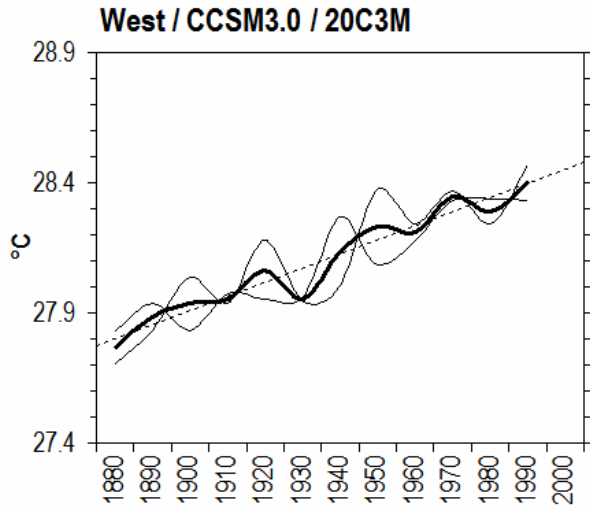
508 are listed in Table 2. Triangles represent corresponding values from the NOAA OI v.2 data set.

509 The decade marked 2000 includes January 2000 through December 2005.



510

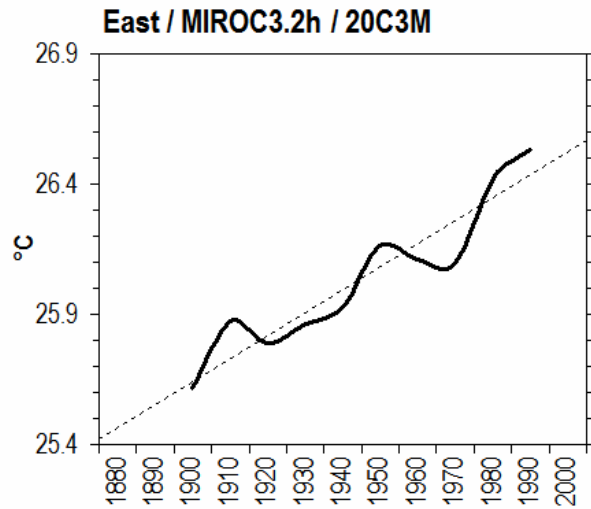
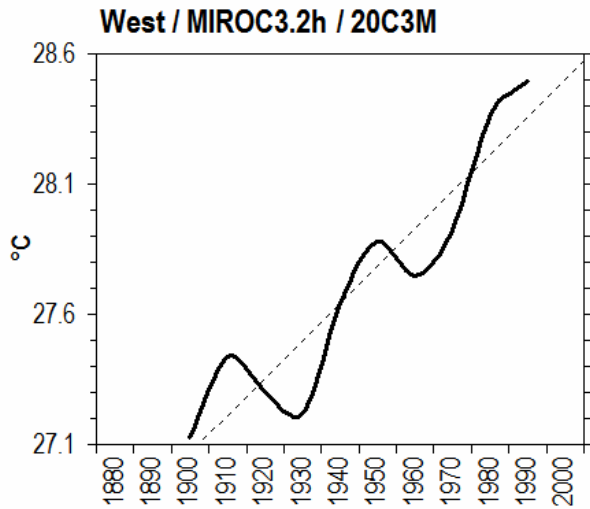
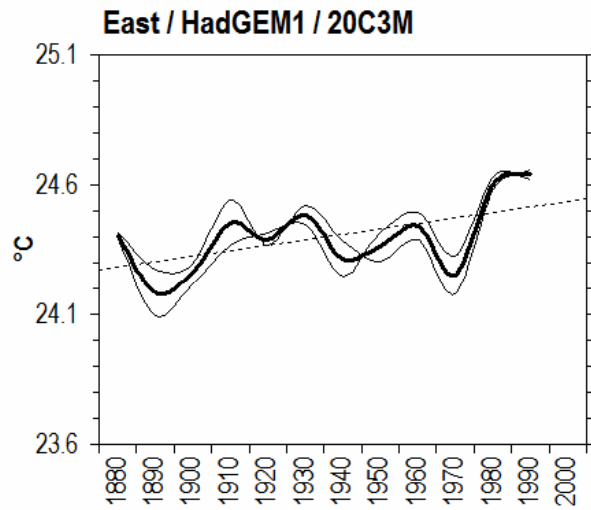
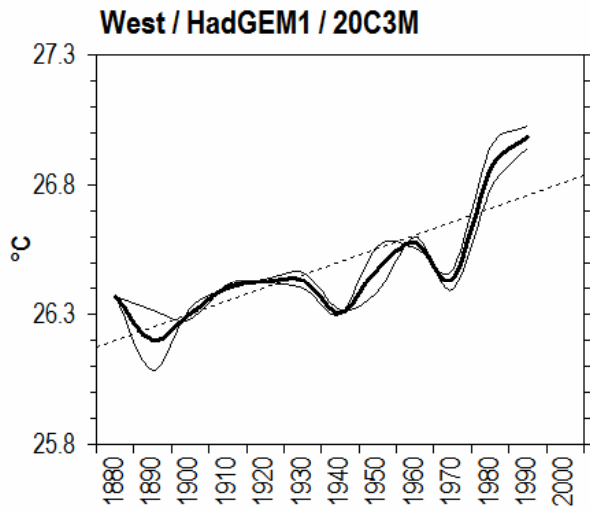
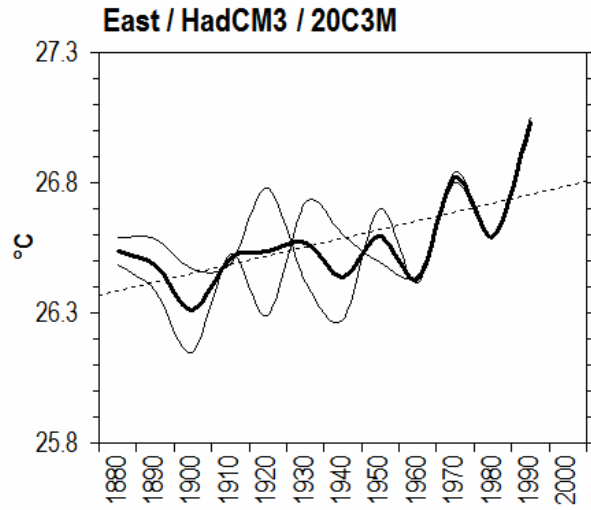
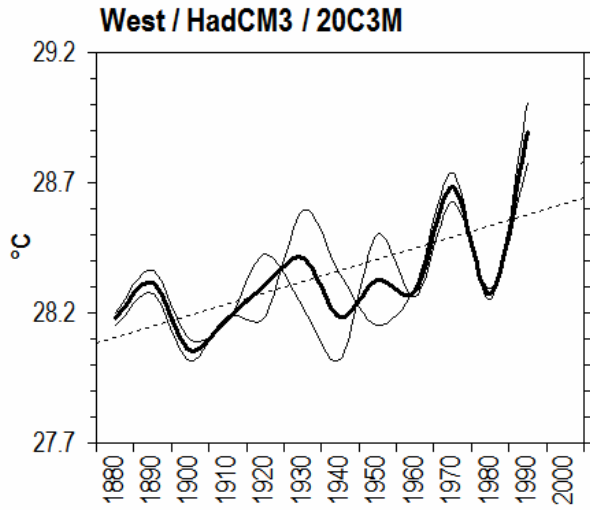
511 **Figure 3.** Time series of observed decadal mean equatorial Pacific zonal SST gradient ( $^{\circ}\text{C } ^{\circ}\text{lon}^{-1}$ ) from HadISST1 (left) and NOAA ERSST v.3 (right). Dashed lines represent linear trends, the  
 512  $^{\circ}\text{C } ^{\circ}\text{lon}^{-1}$ ) from HadISST1 (left) and NOAA ERSST v.3 (right). Dashed lines represent linear trends, the  
 513 magnitudes and significance of which are listed in Table 2. Triangles represent corresponding  
 514 values from the NOAA OI v.2 data set. The decade marked 2000 includes January 2000 through  
 515 December 2005.



Decade

Decade

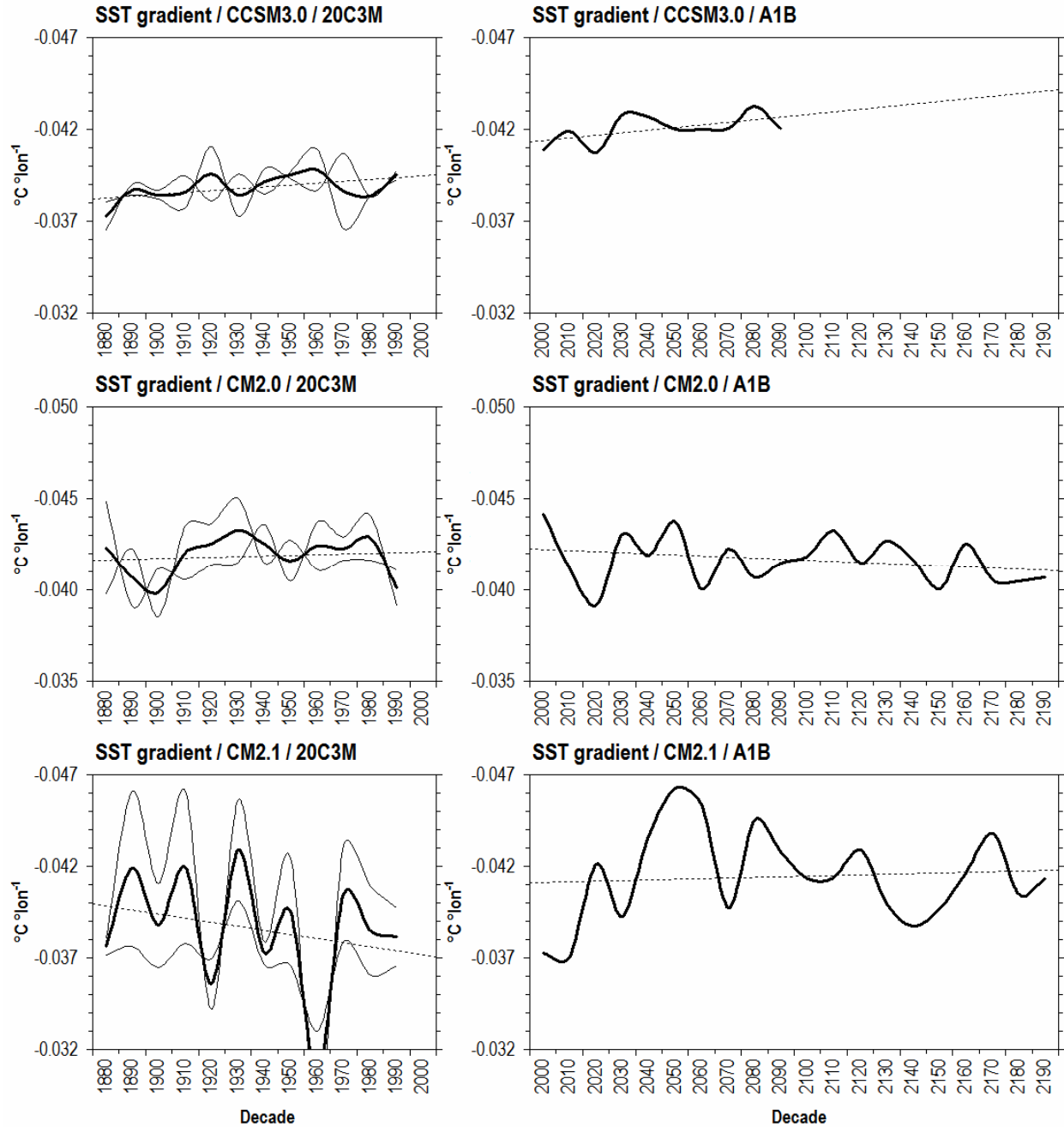
517 **Figure 4.** Time series of simulated decadal mean SST ( $^{\circ}\text{C}$ ) in the western (left column) and  
518 eastern (right column) equatorial Pacific Ocean from the 20C3M experiment of the CCSM3.0  
519 (top row), CM2.0 (middle row), and CM2.1 (bottom row). Thin lines are individual realizations,  
520 and the heavy line is the mean. Dashed lines represent linear trends of the means.



Decade

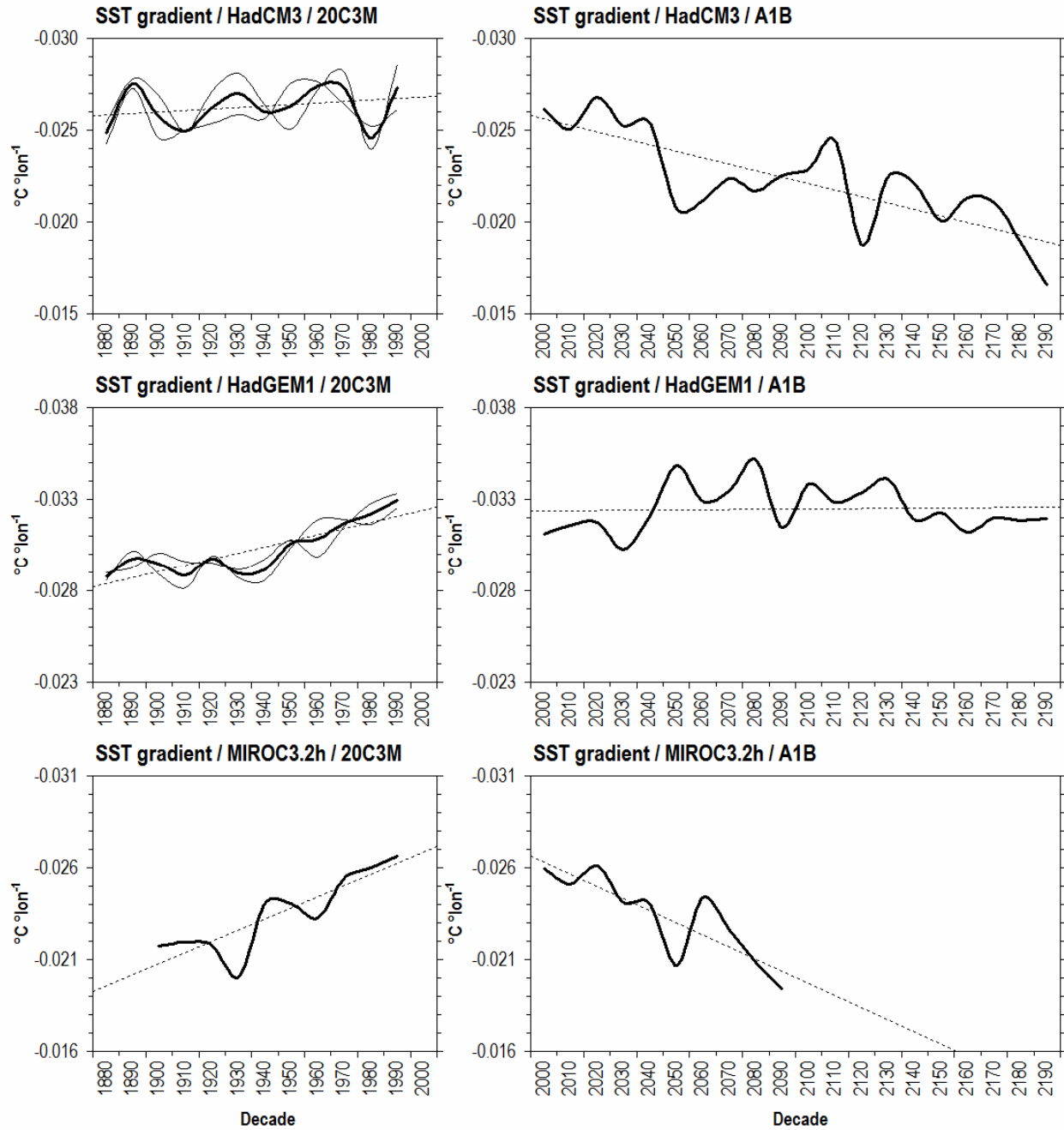
Decade

522 **Figure 5.** As in Figure 4 but of the HadCM3 (top row), HadGEM1 (middle row), and  
523 MIROC3.2h (bottom row).



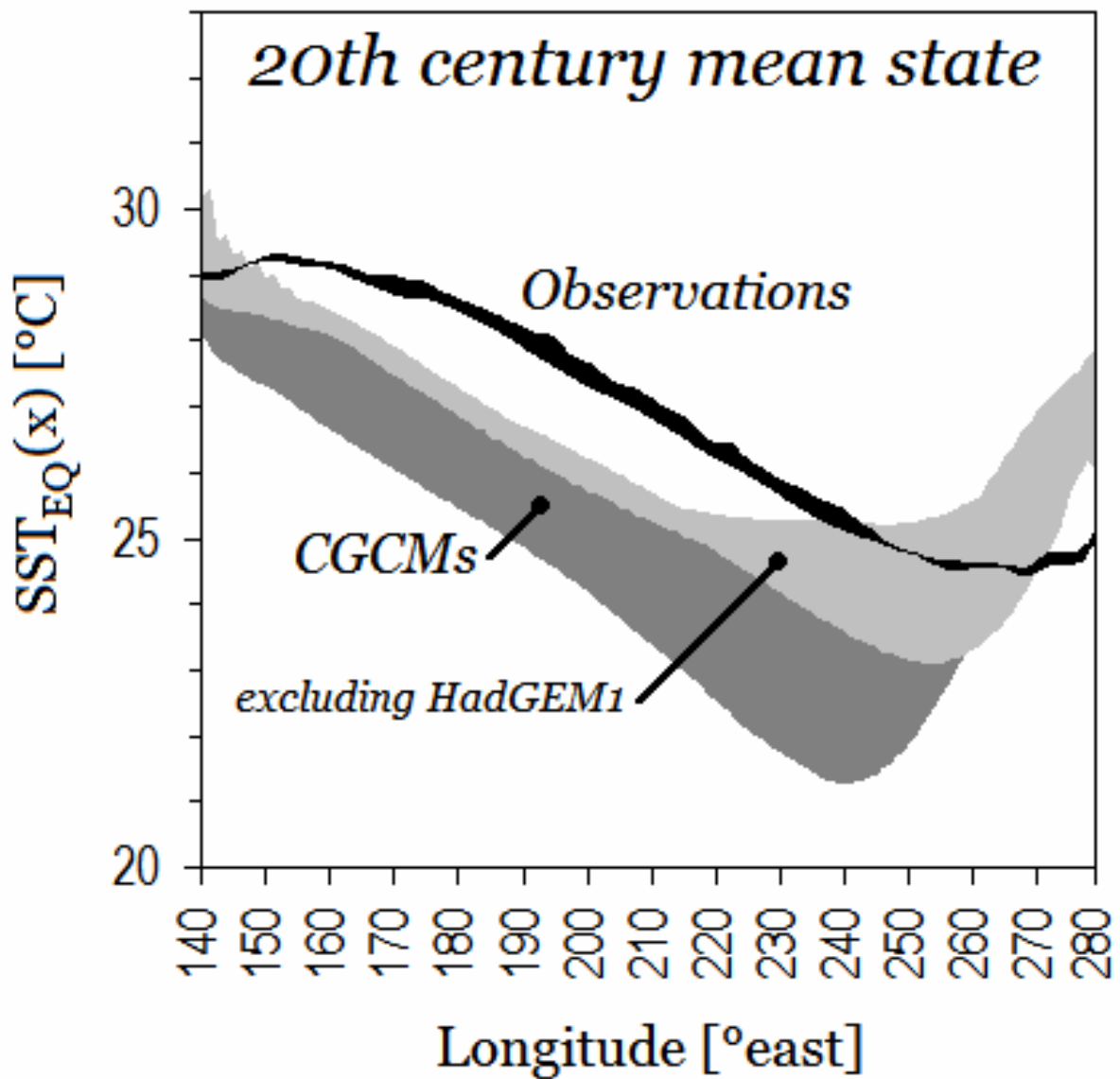
524

525 **Figure 6.** Time series of simulated decadal mean equatorial Pacific zonal SST gradient ( $^{\circ}\text{C } ^{\circ}\text{lon}^{-1}$ )  
 526  $^{\circ}\text{C } ^{\circ}\text{lon}^{-1}$ ) from the 20C3M (left column) and SRES-A1B (right column) experiments of the CCSM3.0  
 527 (top row), CM2.0 (middle row), and CM2.1 (bottom row). Thin lines are individual realizations,  
 528 and the heavy line is the mean. Dashed lines represent linear trends of the means.



529

530 **Figure 7.** As in Figure 6 but of the HadCM3 (top row), HadGEM1 (middle row), and  
 531 MIROC3.2h (bottom row).



532

533 **Figure 8.** Range of observed (HadISST1 and NOAA ERSST v.3; black) and model simulated  
 534 (gray) mean equatorial SST (averaged from 2.5°S to 2.5°N; °C) as a function of longitude (°east)  
 535 over the twentieth century (January 1900 through December 1999). The light and dark grays  
 536 together represent the range from all six CGCMs analyzed in the present study, and the light gray  
 537 represents the range if HadGEM1 is excluded.